Published in final edited form as:

Cell Rep. 2017 June 20; 19(12): 2598–2612. doi:10.1016/j.celrep.2017.05.089.

Ptbp2 controls an alternative splicing network required for cell communication during spermatogenesis

Molly M. Hannigan[1], **Leah L. Zagore**[1], and **Donny D. Licatalosi**[1,2,*]

[1]Center for RNA Science and Therapeutics, Case Western Reserve University, Cleveland, Ohio, 44106, USA

Summary

Alternative splicing has essential roles in development. Remarkably, spermatogenic cells express more alternatively spliced RNAs compared to most whole tissues, however regulation of these RNAs remains unclear. Here, we characterize the alternative splicing landscape during spermatogenesis, and reveal an essential function for the RNA binding protein Ptbp2 in this highly regulated developmental program. We found that Ptbp2 controls a network of genes involved in cell adhesion, migration, and polarity, suggesting that splicing regulation by Ptbp2 is critical for germ cell communication with Sertoli cells (multifunctional somatic cells necessary for spermatogenesis). Indeed, *Ptbp2*-ablation in germ cells resulted in disorganization of the F-actin cytoskeleton in Sertoli cells, indicating that alternative splicing regulation is necessary for cellular crosstalk during germ cell development. Collectively, the data delineate an alternative splicing regulatory network essential for spermatogenesis, the splicing factor that controls it, and its biological importance in germ-Sertoli communication.

eTOC Blurb

[*]To whom correspondence should be addressed, Donny D. Licatalosi, Center for RNA Science and Therapeutics, Case Western Reserve University, Cleveland, OH, 44106, USA, Tel: (216) 368-4757, Fax: (216) 368-2010, ddl33@case.edu.
[2]Lead Contact

Author Contributions

M.M.H, and L.L.Z conducted the experiments. M.M.H and D.D.L designed the experiments, analyzed the data, and wrote the manuscript.

Accession Numbers

Raw and processed RNA-Seq and HITS-CLIP datasets generated in this study are available at NCBI (GSE79106).

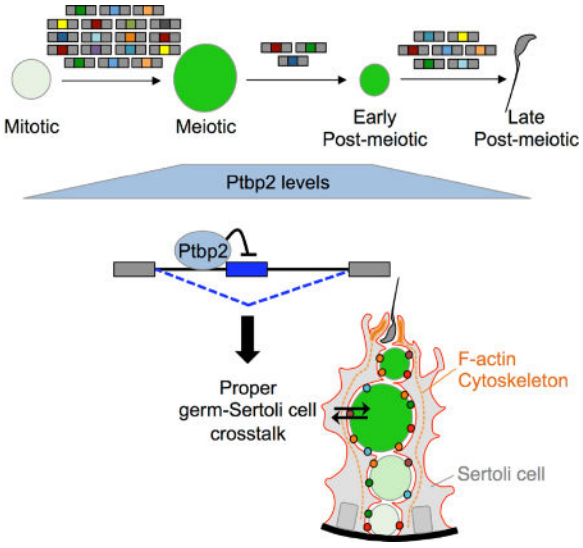

Hannigan et al. characterize the alternative splicing landscape during spermatogenesis and reveal an essential role for Ptbp2 in this temporal regulation. Moreover, splicing regulation by Ptbp2 is required for proper regulation of trafficking and cell polarity genes, and cell communication during germ cell development.

Keywords

post-transcriptional regulation; spermatogenesis; cell-cell communication; alternative splicing; RNA networks

Introduction

Mammalian spermatogenesis is arguably one of the most complex developmental programs. This process involves three main phases: 1) a mitotic phase when spermatogonia proliferate and differentiate, 2) a meiotic phase when DNA recombination occurs in spermatocytes and haploid spermatids are formed, and 3) a post-meiotic differentiation phase in which round spermatids elongate, condense, and are released into the seminiferous tubule lumen as spermatozoa. During their development, germ cells must remain in contact with Sertoli cells (multifunctional somatic cells that are essential for spermatogenesis) (Griswold, 1998).

Alternative splicing (AS) plays a major role in increasing transcriptome complexity and its dysregulation is associated with multiple human diseases (Scotti and Swanson, 2016). Strikingly, the testis ranks among top tissues with respect to the number of AS mRNA variants (Soumillon et al., 2013; Ramskold et al., 2009). In fact, the complexity of mRNA isoforms in spermatogenic cell types exceeds that of most whole tissues (Soumillon et al., 2013). It remains unclear why AS is robust in these cell types, the extent to which these AS mRNAs are controlled developmentally, and the roles of different RNA binding proteins (RBPs) in their regulation (Kleene, 2013; Licatalosi, 2016).

Ptbp2, a member of the PTB (polypyrimidine-tract binding) family of RBPs (Sawicka et al., 2008), is a strong candidate to function as a regulator of AS during spermatogenesis. PTB proteins bind CU-rich elements proximal to specific AS exons and can repress splicing via competition with the U2AF splicing factor (Sharma et al., 2005), interference with spliceosome assembly via interaction with U1 snRNA (Sharma et al., 2011), and occlusion of splice sites via PTB-multimerization or looping of RNA sequences (Oberstrass et al., 2005).

The two best-studied PTB proteins, Ptbp1 and Ptbp2 have mostly inverse patterns of expression in different tissues and developmental stages, and regulate the splicing of overlapping but non-redundant sets of RNA targets (Lillevali et al., 2001; Polydorides et al., 2000; Makeyev et al., 2007; Boutz et al., 2007; Spellman et al., 2007; Vuong et al., 2016). The biological impact of PTB proteins is best understood in the nervous system, where switches in Ptbp1 and Ptbp2 levels dictate temporal control of AS (Boutz et al., 2007; Makeyev et al., 2007; Licatalosi et al., 2012; Zheng et al., 2012; Li et al., 2014).

Ptbp1 and *Ptbp2* also display stage-specific expression differences in postnatal germ cells (Xu and Hecht, 2007; Schmid et al., 2013; Zagore et al., 2015). Ptbp1 dominates in mitosis but decreases in meiotic spermatocytes. Conversely, Ptbp2 significantly increases in spermatocytes and persists until the elongating steps of spermatid differentiation. Whether Ptbp2 functionally replaces Ptbp1, or if the Ptbp1 to Ptbp2 switch is important for stage-specific AS regulation during spermatogenesis is unknown.

We previously observed that *Ptbp2* ablation results in spermatogenetic arrest (Zagore et al., 2015), with features that resemble mouse knockouts of genes that have roles in germ-Sertoli cell communication (e.g., Cadm1, Basigin, Fndc3a) (Bi et al., 2013); (Obholz et al., 2006) (van der Weyden et al., 2006; Yamada et al., 2006). Here, we used RNA-Seq and HITS-CLIP to understand the underlying molecular basis for germ cell arrest in Ptbp2-deficient cells. We demonstrate that Ptbp2 is required for AS regulation for over 200 genes, directly binds AS targets to repress splicing, and controls AS changes that occur between mitotic and meiotic germ cells. Strikingly, our data reveal a critical role for Ptbp2 in regulating the splicing of a network of genes important for germ-Sertoli cell communication. Furthermore, we demonstrate that germ cell-specific dysregulation of this AS network, results in disorganization of the actin cytoskeleton in Sertoli cells. Collectively, the data define, for the first time, a critical AS regulatory network in spermatogenesis.

Results

Dynamic regulation of AS in different stages of spermatogenesis

To investigate the dynamics and regulation of AS in different stages of spermatogenesis, we analyzed RNA-Seq datasets previously generated from four spermatogenic cell types (spermatogonia, spermatocytes, round spermatids, and spermatozoa) (Soumillon et al., 2013). RNA-Seq reads were mapped with OLego and processed with Quantas to measure AS of cassette exons (CASS), tandem exons spliced in a coordinated or mutually exclusive manner (TAND or MUTX, respectively), differences in 5’ and 3’ splice site (SS) selection (ALT5 or ALT3, respectively), and changes in intron retention (IRET) (Wu et al., 2013; Yan

et al., 2015). Pairwise comparisons of AS isoform levels were performed in spermatogonia versus spermatocytes (transition 1 or T1; mitotic versus meiotic), spermatocytes versus round spermatids (transition 2 or T2: meiotic versus post-meiotic), and round spermatids versus spermatozoa (transition 3 or T3) (Figure 1A). Spermatozoa are transcriptionally inert and contain transcripts made during spermatid elongation (Johnson et al., 2011), thus T3 can be considered a comparison between early versus late post-meiotic cells. For all comparisons, differences in AS isoforms were expressed as the change in percent spliced in, or ΔPSI (Figure 1A).

In total, 1,030 AS changes of at least 20% (ΔPSI>20) were identified in transcripts derived from 712 genes (Figure 1A–C; File S1) with only 16% of these genes showing stage-specific changes in more than one transition (Figure 1C). Examination of individual alternative exons showed that 108 were regulated in more than one transition (Figure 1D), with the majority (94/108) temporarily switching AS isoform ratios before reverting to PSI values present at earlier developmental stages (Figure 1E).

Stage-specific changes were measured by RT-PCR analysis of testes collected at postnatal day 6 (P6), P19, or P25 (when the most advanced germ cells present are mitotic spermatogonia, meiotic spermatocytes, and post-meiotic spermatids, respectively) (Figure 1F; Figure S1A). Importantly, ΔPSI values derived from RNA-Seq of isolated cells had a positive correlation with ΔPSI values calculated from RT-PCR analysis of whole testis (R=0.71, 24 targets examined), thus validating the analysis (Figure S1B; File S1).

Despite comparable numbers of RNA-Seq reads (Table S1), distinct differences in the number and magnitude of AS changes were observed for each transition. Nearly 75% of AS changes occurred in Tl (Figure 1B,E) affecting 595 genes. The fewest AS changes and smallest range of ΔPSI values occurred in T2, followed by an increase in the number and magnitude of AS events in T3 (Figure 1B–D, G, H). Re-examination of the RNA-Seq data using different mapping and AS quantification tools (TopHat (Trapnell et al., 2012) and MATS (Shen et al., 2012), respectively) confirmed these biases in stage-specific AS (Figure S2).

These observations define distinct stage-specific programs of AS isoform regulation, with the greatest impact on the germ cell transcriptome as cells transit from the mitotic to meiotic stages of spermatogenesis. Subsequently, AS isoforms are generally maintained during the meiotic and early post-meiotic stages, before diverging during spermatid differentiation.

Ptbp2 is required for AS regulation in meiotic germ cells

Ptbp2 levels increase when the greatest AS changes occur. To investigate if Ptbp2 is controlling AS during spermatogenesis, we generated RNA-Seq datasets from wild type (WT) and *Ptbp2* conditional knockout (cKO) testes at P25. At this age, the majority of germ cells are in the post-meiotic stage, and spermatogenic defects are detectable in only a subset of cKO seminiferous tubules (Zagore et al., 2015).

Our analysis identified 257 AS differences in RNAs from 217 genes (ΔPSI≥20%; Figure 2A,B; File S1). AS changes were confirmed by RT-PCR, with a positive correlation with

ΔPSI values derived from RNA-Seq (R=0.76; Figure 2C; Figure S3A; File S1). Notably, the majority of the AS changes for the 217 genes had negative ΔPSI values indicating that Ptbp2 was required for more exon repression events in testes compared to exon activation (163 blue and 94 red, respectively, Figure 2B). The 217 genes showed a strong concordance in RNA levels in WT and cKO testes (R=0.93; Figure 2D), with 81.1% showing no statistically significant difference. As expected, genes that did differ in RNA abundance were predominantly those with differences in intron retention (R=0.37; Figure 2B). We conclude that Ptbp2 is required for AS regulation in the testis, and that the majority of the Ptbp2-dependent AS events affect the primary sequence of the encoded proteins rather than altering total transcript abundance.

Independent of AS changes, we performed a differential gene expression analysis and identified 988 genes that differed in steady state mRNA levels between WT and cKO testes; nearly all having reduced levels in cKO testes (93.6%, 925/988; Figure 2E, inset; File S2). Notably, the distribution of fold-change values varied between genes that showed increased RNA levels versus those that decreased. More specifically, genes with reduced RNA levels in cKO were accompanied by much larger fold changes (Figure 2E, red versus black line). Strikingly, genes with the lowest RNA levels in cKO testes were those robustly expressed in spermatids, including the transition protein genes *Tnp1* and *Tnp2*, and the protamine genes *Prm1* and *Prm2* (Figure 2E) (Kleene, 2013). Therefore, we asked whether the lopsided difference in RNA levels was due to the absence of spermatid-expressed transcripts in cKO testes. Using RNA-Seq data from purified germ cells (Soumillon et al., 2013), we found that the vast majority of genes with RNA differences in cKO testes had a significant RNA difference between purified spermatocytes and round spermatids (94%). In fact, nearly all genes with decreased RNA levels in cKO testes had increased RNA levels in spermatids (Figure 2F, top right). Thus, we conclude that early post-meiotic arrest accounts for the deficits in specific RNAs in cKO testis.

The dearth of spermatid-expressed transcripts in P25 cKO testes, along with the few AS differences between spermatocytes and round spermatids (i.e., T2), suggests that the majority of the AS differences in cKO testes reflect Ptbp2-dependent splicing events in meiotic germ cells. To explore this further, we measured AS isoforms in testes collected prior to P25. Importantly, AS changes were confirmed at earlier time points, including P19 when the most advanced germ cells are in prophase of meiosis I (Figure 2G; Figure S3B). Collectively, these observations suggest that the majority of AS changes in cKO testes occur in meiotic spermatocytes.

Ptbp2 is required for stage-specific AS regulation during spermatogenesis

Since Ptbp2 levels increase during T1 and is required for AS regulation in meiotic germ cells, we examined the overlap between AS differences identified in T1 and cKO testes. Comparison of AS cassette exons in both datasets identified a common set of 250 exons (Figure 3A). As expected, the RNA-Seq ΔPSI values from purified cells were larger than ΔPSI values from whole testes, owing to cellular heterogeneity of the latter (Figure 3B). Regardless, the ΔPSI values showed a positive correlation (R=0.53). Strikingly, the majority of enhanced cassette exons in meiotic cells were spliced in a Ptbp2-dependent manner,

whereas the majority of cassette exons with decreased splicing in meiotic cells were repressed in a Ptbp2-dependent manner. From these observations, we conclude that increased expression of Ptbp2 in meiotic cells promotes over 25% of the splicing changes that occur as germ cells progress from the mitotic to meiotic stages of spermatogenesis.

Ptbp2 levels are maintained during T2 (where the fewest and smallest AS changes occur), and decline in T3. Therefore, we examined the overlap between AS differences in T3 and cKO testes to examine how reduction of Ptbp2 levels may impact AS changes in post-meiotic spermatids. Notably, the 51 cassette exons common to T3 and cKO displayed an inverse relationship compared to overlapping exons in T1 and cKO (Figure 3C, D; R= −0.41). More specifically, the majority of cassette exons with increased splicing in T3 were repressed by Ptbp2, whereas the majority of cassette exons with decreased splicing in T3 were enhanced by Ptbp2. Collectively, these observations indicate that Ptbp2 levels influence stage specific AS during spermatogenesis.

The Ptbp2-RNA interaction map shows recurrent and direct binding to repressed exons

RBPs can function as both splicing enhancers and repressors depending on where they bind relative to an AS exon (Licatalosi and Darnell, 2010; Konig et al., 2011; Fu and Ares, 2014). To generate a transcriptome-wide map of Ptbp2-RNA interactions in spermatogenic cells, we used HITS-CLIP (Licatalosi et al., 2008). We isolated and sequenced 30–50 nucleotide RNA fragments that were cross-linked to and co-immunoprecipitated with Ptbp2 from three adult testes (Figure 4A). After mapping and filtering the libraries individually, the resulting CLIP tags were merged to identify reads common to all three libraries, hereafter called BR3 clusters (biologically reproducible in 3/3 animals). BR3 clusters were broadly distributed across the germ cell transcriptome, with ~70% mapping to 5,396 annotated RefSeq genes and the majority residing in introns (Figure 4B; File S3). Consistent with functional and structural studies of PTB-RNA interactions (Oberstrass et al., 2005; Spellman and Smith, 2006; Keppetipola et al., 2012), the most enriched sequences within BR3 clusters were CU-rich motifs (Figure 4C,D).

To assess the distribution of Ptbp2-RNA interactions near Ptbp2-dependent AS events, we focused on cassette exons flanked by constitutively spliced exons. Of the 67 AS exons with ΔPSI>20, 25 exons had positive ΔPSI values (more abundant exon inclusion in WT) and 42 had negative ΔPSI values (more abundant exon inclusion in cKO). Approximately 67% of the examined regions contained reproducible (BR2 or BR3) Ptbp2-RNA interactions (15/25 Ptbp2-enhanced and 32/42 Ptbp2-repressed exons); however, the distribution and conservation of binding sites in these regions were markedly different (Figure 5). Ptbp2-RNA interactions associated with enhanced exons were broadly distributed, with only 7 exons having Ptbp2 bound within 500 bases of the 3’ or 5’ SS of the AS exon (Figure 5A,B). In contrast, the majority of repressed exons had Ptbp2-RNA interactions proximal to the AS exon, with the greatest concentration near the 3’SS (Figure 5D,E). In addition to this positional bias, Ptbp2-bound sequences associated with repressed exons had higher conservation scores (Figure 5C). Ptbp2-binding sites were also examined across sequences associated with a control set of 100 randomly selected constitutively spliced exons, with no identifiable enrichment or positional bias in Ptbp2 binding observed (Figure 5F). The

increased density of Ptbp2-interactions near repressed exons and the high conservation of these binding sites are consistent with existing models of splicing repression by PTB proteins derived from *in vitro* assays and experiments in cell culture (Keppetipola et al., 2012). Taken together, our RNA-Seq and CLIP data suggest that Ptbp2 is required for regulation of AS isoforms in spermatogenesis via a series of primary (direct) and secondary (indirect) targets.

Ptbp2 regulates AS of a network of trafficking and cell polarity genes

Having established that Ptbp2 governs AS patterns in spermatogenesis, we examined the functions of 217 genes (ΔPSI≥20 in WT versus cKO) to gain insights into the molecular basis underlying the cKO germ cell defects. Literature searches, database mining, and informatics approaches showed that a large cohort of these genes encode proteins that are functionally related and directly interact with one another (Figure 6; Figure S4A). More specifically, analysis of gene ontology (GO) annotations assigned the majority (83%) to enriched terms that clustered into 7 related groups based on biological process (Groups 1–3), molecular function (Groups 4,5) and cellular component (Groups 6,7) (Figure 6A; File S4).

Group 1 contained a large set of genes encoding proteins with roles in membrane organization and protein transport. Strikingly, several Group 1 genes encode interacting proteins that function in nearly all steps of vesicle-mediated trafficking (Figure S4A). Examples include subunits of the AP-1 and AP-2 adaptor protein complexes involved in cargo selection and vesicle formation (Ap1b1, Ap2a1, Ap2a2), and Dennd1a which is a component of clathrin-coated vesicles that directly bind the AP-2 adaptor protein complex (Marat et al., 2011). Also represented were proteins that function in vesicle tethering to microtubules, and docking and fusion of vesicles with target membranes (e.g., Snap23, Synj1, Synj2, Rims2, Eps15). Genes encoding proteins that bind to and regulate actin dynamics (e.g., Ablim3, Epb4.1, Fhod1, Fmnl1) were listed as well. Among these were genes that comprise Group 2, which represents a single annotation term ‘actin-filament based process’. In fact, there was considerable gene overlap across all enriched terms (Figure 6B,C).

Groups 3 and 4 consisted of genes encoding proteins involved in cell signaling, cell-cell communication, and GTPase regulation. Among the list include multiple guanine nucleotide exchange factors (GEFs) and GTPase activating proteins (GAPs) that regulate signaling and cytoskeletal remodeling events (e.g., Arhgef7, Iqgap1, Myo9b, Rangap1, Rapgef1). Although not assigned to Groups 3 or 4, additional proteins with related functions were identified in the set of 217 genes, including Rab28 (a GTPase), Wdr7, and Fam116B.

Group 5 contained general terms related to binding, as well as more specific terms ‘SH3 domain binding’ and ‘cytoskeletal protein binding’. Notably, all of the genes in the ‘SH3 binding domain’ subgroup encoded proteins that bind AP-1 and AP-2 complexes, or regulate the actin cytoskeleton. Similarly, genes in the ‘cytoskeletal protein binding’ subgroup were present in Group 1 and encode proteins that regulate actin dynamics.

Consistent with our enrichment analysis, the majority of genes with AS changes in cKO testes encoded proteins that reside in the cytoplasm (Group 6), or localize to clathrin coated

vesicles, the plasma membrane, and cell-cell junctions (Group 7). Examples of the latter include proteins that couple membrane and cytoplasmic proteins at sites of adhesion (e.g, Afadin, Enah, Grip1, Sorbs1).

The data indicate that Ptbp2 is required for coordinate AS control of a functionally coupled network of genes. Determining how these AS changes impact germ cell functions individually and in aggregate will require further study. However, we identified several AS changes that alter annotated domains, including: 1) an exon in Dctn1 that introduces 3 threonines that control localization and microtubule binding (Zhapparova et al., 2013), 2) exons that alter calponin homology domains in Ehbp1l1 and Lrch3, as well as a transmembrane domain in the latter (based on UniProt annotations, (The UniProt Consortium, 2016)), 3) the basic region of the DAD domain in Fmnl1, which has a key role in the regulatory mechanism that controls actin remodeling (Wallar et al., 2006; Kühn and Geyer, 2014), and 4) an exon that introduces a premature termination codon that leads to decreased levels of Iqgap1, an effector for the Rho GTPase Cdc42 (Watanabe et al., 2015). In the testis, interactions between Iqgap1 and Cdc42 are believed to regulate Sertoli-germ cell adherens junction dynamics (Lui et al., 2005). Interestingly, we observed that Ptbp2 directly bound to and was required for correct expression of AS isoforms of Cdc42 (Figure S4B). More specifically, Ptbp2-deletion resulted in a shift in the levels of Cdc42 AS isoforms previously shown to have distinct functional roles in regulating polarity of primary neurons (Yap et al., 2016).

Altogether, our data indicates that *Ptbp2*-deletion disproportionately affects the expression of AS isoforms from a network of functionally related genes with roles in membrane remodeling, protein trafficking, cytoskeletal reorganization, and GTPase-mediated signaling. These inter-related processes orchestrate cell polarity, adhesion, migration, and cell-cell communication (Mellman and Nelson, 2008; Parsons et al., 2010; Cheng et al., 2011; West and Harris, 2016), suggesting that such functions may be perturbed in cKO testes.

Loss of Ptbp2 in germ cells disrupts the Sertoli cell cytoskeleton

As germ cells migrate toward the lumen during spermatogenesis they must remain in intimate contact with Sertoli cells. This interaction depends on membrane protein remodeling and signal transduction cascades to maintain cell polarity and adhesion (Cheng et al., 2011). Based on our findings and the phenotypic features of cKO testes, we hypothesized that Ptbp2 is essential for proper adhesion and/or crosstalk between germ and Sertoli cells.

Pharmacologic disruption of germ-Sertoli cell adhesion or ablation of signaling and polarity proteins cause disorganization of the Sertoli cell cytoskeleton (Tanwar et al., 2011; Tanwar et al., 2012; Dong et al., 2015; Tang et al., 2016). To test the hypothesis that *Ptbp2*-deletion in germ cells impacts cytoskeletal organization in Sertoli cells, fluorescence microscopy was performed with phalloidin to stain filamentous actin (F-actin). Sections were counterstained with PNA to classify spermatids and identify tubules with similar cell compositions (Nakata et al., 2015). As expected (Vogl et al., 2008; Johnson, 2014), F-actin was readily detected at the interface between elongated spermatids and Sertoli cells in P36 WT testes (Figure 7A–D, open arrows), with little to no F-actin associated with round spermatids (Figure 7A–B,

closed arrows). Also evident were polarized linear stalks of F-actin extending from the basal membrane to the lumen (Figure 7A, arrowheads), as previously described (Tang et al., 2016). Despite the absence of elongated spermatids, an abundance of F-actin was detected in the apical region of cKO tubules, with the greatest accumulations in regions devoid of germ cell nuclei (Figure 7E–G). In addition, F-actin tracks extending towards the lumen were more intensely stained in cKO tubules (Figure 7E,G, Figure S5A–F,R; arrowheads). Similar patterns of excess F-actin were also observed in nearly all seminiferous tubules in P24 cKO testes (Figure 7K–M) including those where the first wave of germ cells have not yet completed meiosis (Figure S5G–L,Q), suggesting that disorganization of the actin cytoskeleton is not an indirect consequence of spermatid arrest and premature detachment. Importantly, co-immunostaining for the germ cell marker Ddx4, indicated that aberrant F-actin was not in germ cells (Figure S5M–P). These observations demonstrate that ablation of Ptbp2 in male germ cells results in disorganization of the F-actin cytoskeleton in Sertoli cells. Thus, our data suggest that AS regulation by Ptbp2 in germ cells is essential for germ-Sertoli cell crosstalk, providing new insights into the physiological importance of AS in the testis.

Discussion

While the prevalence of AS isoforms in germ cells has long been known (Yeo et al., 2004; Clark et al., 2007; Ramskold et al., 2009), the dynamics, regulation, and function of AS during spermatogenesis have remained largely unexplored. In this report, we provide new data to significantly advance our knowledge of each of these aspects.

Alternative splicing is regulated in a stage-specific manner during spermatogenesis

Our analysis of available RNA-Seq data identified over one thousand stage-specific AS changes in germ cells isolated at different stages of the first wave of spermatogenesis. The extent to which AS programs may differ during steady state spermatogenesis remains to be determined, however our analysis significantly increases the number of known genes and molecular pathways that are impacted by AS in the male germline. Unexpectedly, the majority of these changes occur when germ cells progress from the mitosis to meiosis phase, followed by a period where AS isoform levels are maintained until the differentiation stage of post-meiotic spermatids. Despite the diverse array of functions ascribed to proteins encoded by genes with stage-specific AS, the majority of the genes in T1 and T3 (512/595 and 137/164, respectively) clustered into enriched categories of GO terms (File S4). Interestingly, when different subgroups of genes were examined, distinct sets of enriched GO annotations were evident between genes with positive or negative PSI values in each transition. For example, genes with repressed AS events in T1 were enriched for terms associated with RNA processing and intracellular transport, whereas AS events that are enhanced in T1 were enriched for genes with roles in mRNA translation (File S4). Accordingly, stage-specific AS in germ cells is predicted to impact several processes through coordinate regulation of multiple components of macromolecular complexes and cellular pathways.

While additional study is required to understand precisely how stage-specific AS events are regulated by different RBPs and their impact on germ cell development, our immediate goal was to set the stage for assessing the role of Ptbp2 in AS regulation during spermatogenesis. Notably, changes in Ptbp2 levels coincide with germ cell stages that exhibit the greatest AS changes (T1 and T3), whereas the fewest and smallest AS differences occur in T2, when Ptbp2 levels are largely maintained. By comparing AS changes in different transitions with those in Ptbp2 cKO mice, we found a striking relationship between exons with stage-specific changes and Ptbp2-dependent regulation. More specifically, cassette exons with increased or decreased splicing in T1 (when Ptbp2 levels increase) were predominantly enhanced or repressed by Ptbp2, respectively. Conversely, cassette exons with increased or decreased splicing in T3 (when Ptbp2 levels decline) were generally repressed or enhanced by Ptbp2, respectively. We cannot exclude the possibility that spermatid arrest contributes to AS differences between P25 WT and cKO testes. However, the data suggests that any such contribution is likely to minor, as few AS changes exist between spermatocytes and spermatids, and the majority of genes with AS changes in cKO testes do not display significant differences in overall RNA levels. Importantly, splicing changes in cKO testes could be detected when the most advanced germ cells are in prophase of meiosis I. Collectively, our data indicates a role for Ptbp2 as a critical regulator of stage-specific AS isoforms during spermatogenesis.

Ptbp2 controls alternative splicing in germ cells through direct and indirect interactions

CLIP analysis showed Ptbp2 binds CU-rich sites across the germ cell transcriptome. Interestingly, the majority had low conservation scores, and those that mapped to introns were generally positioned far from 5’ or 3’SS (Figure S6). The prevalence of these interactions may explain the high levels of Ptbp2 in the nucleus (Xu and Hecht, 2007), which may serve to prevent sequestration of Ptbp2 at sites with minimal regulatory potential. While Ptbp2 mostly binds intronic sequences, binding sites in coding and non-coding exonic regions are also observed, raising the possibility that Ptbp2 may have splicing-independent roles in post-transcriptional regulation in germ cells. Additional experiments using tissue with less cellular heterogeneity (earlier time points) or purified cell types are needed to explore this possibility further.

In contrast, our data support a role for Ptbp2 as a regulator of AS in spermatogenic cells. We found that Ptbp2 binds proximal to the 3’SS and/or within the AS exon to repress splicing, while interactions associated with Ptbp2-enhanced exons lacked a positional bias. Consistent with AS regulation by tissue-restricted RBPs (Merkin et al., 2012), binding sites associated with repressed exons also had higher conservation scores. These observations parallel extensive biochemical and reporter-based assays supporting a direct role for PTB proteins as splicing repressors, while also suggesting that Ptbp2 regulates AS isoforms in the testis via a combination of primary and secondary targets.

Notably, several post-transcriptional regulators including Clk4, Srsf14, Elavl2, Pum2, and Csda/Ybx3 are alternatively spliced in cKO testes, indicating that a subset of AS changes likely result from alterations in these factors and their respective downstream targets. Loss of Ptbp2 may also expose sites that can be recognized by other RBPs and/or alter RNA

structure, leading to widespread redistribution of RBP-RNA interactions. The extent to which Ptbp2 functions in cooperation with or to antagonize other RBPs proposed to have roles in AS regulation in spermatogenesis including Rbm5 (O'Bryan et al., 2013), Sam68 (Sette et al., 2010), T-STAR (Ehrmann and Elliott, 2010), and Celf1 (Kress et al., 2007) remains to be determined.

The impact of Ptbp2 loss on cellular structures during spermatogenesis

Tissue-restricted RBPs generally fine-tune AS isoform ratios for large cohorts of genes rather than exerting dramatic splicing changes on a limited set (Licatalosi and Darnell, 2010; Fu and Ares, 2014). This mode of regulation allows distinct pools of alternative protein isoforms to be produced in a given cell, and therefore modulate ubiquitous cell functions in different cellular contexts. Using a conservative ΔPSI cutoff, we discovered that a disproportionate number of AS genes in cKO testes have roles in membrane and cytoskeletal remodeling, protein trafficking, and GTPase-mediated signaling. Notably, GO annotation terms associated with cytoskeletal regulation were enriched among genes with the greatest splicing changes in T1 and T3 (File S4). These observations suggest that AS regulation functions in the dynamic coordination cell adhesion, migration, and polarity during spermatogenesis.

Polarity proteins and actin regulatory factors are thought to have critical roles in maintaining adhesion of Sertoli cells with germ cells during their development and movement towards the lumen (Lie et al., 2010; Cheng et al., 2011). Strikingly, conditional deletion of *Ptbp2* in germ cells resulted in disorganization of F-actin filaments in Sertoli cells, a phenotype previously attributed to loss of Sertoli cell polarity (Tanwar et al., 2011; Tanwar et al., 2012; Dong et al., 2015; Tang et al., 2016). Interestingly, linear F-actin filaments in Sertoli cells have been proposed to facilitate germ cell migration (Tanwar et al., 2011; Tanwar et al., 2012; Dong et al., 2015; Tang et al., 2016).

Our biological and computational analyses of *Ptbp2* deletion in germ cells provide insights into the molecular basis of the cKO spermatogenic defects, which include increased apoptosis and premature release into the lumen. Consequently, our data provide a rationale for why cKO testes resemble gene knockouts of specific membrane proteins and signaling factors (Bi et al., 2013; Obholz et al., 2006; van der Weyden et al., 2006; Yamada et al., 2006).

Our analyses suggest a model whereby Ptbp2 controls a network of AS events in postmitotic germ cells (spermatocytes and spermatids) necessary to establish the correct protein isoforms required for germ-Sertoli cell communication (Figure S7). While it is likely that some AS changes have more deleterious effects than others in male germ cells, we propose that spermatogenic failure in cKO testes results from aberrant accumulation of AS isoforms across the large network of functionally interconnected proteins.

In summary, we demonstrate that AS is highly regulated in the testis, present evidence that this regulation is necessary for spermatogenesis, and define a network of genes with roles in cell adhesion, polarity, and cytoskeletal remodeling that are coordinately regulated by Ptbp2-dependent AS. This data offers important insights into the physiological functions of an AS

program in the mammalian germline, and the opportunity to unravel connections between Ptbp2-dependent AS in different developmental systems.

Experimental Procedures

Animals and tissue collection

To obtain cKO and WT littermate controls, *Stra8-iCre*$^{+/+}$; *Ptbp2*$^{\Delta E4/+}$ males were crossed with *PtbpT*$^{flox/+}$ females as previously described (Zagore et al., 2015). The day of birth was considered postnatal day 0. WT C57BL/6 animals used for validation of stage-specific AS changes. HITS-CLIP libraries were generated from CD-1 animals purchased from Charles River Labs. For all procedures, mice were incapacitated by isofluorane inhalation and sacrificed by cervical dislocation or decapitation. All animal procedures were approved by Institutional Animal Care and Use Committee at CWRU.

RT-PCR

RT-PCR analyses of radiolabelled AS transcripts were performed on biologic replicate samples after determining the optimal cycle number necessary for linear amplification with each primer set, as previously described (Licatalosi et al., 2008). ΔPSI values from RT-PCR analyses were determined after correcting for differences in nucleotide composition (radionucleotide incorporation). Primer pairs used for RT-PCR are listed in Table S3.

RNA-Seq

Paired-end RNA-Seq libraries were prepared from P25 testes from two WT and two cKO animals using Illumina ScriptSeq™ v2 RNA-Seq library preparation kits and sequenced at the CWRU Sequencing Core. Reads were mapped to the mm10 genome with OLego (Wu et al., 2013). The Quantas pipeline was used to infer transcript structure, and quantify alternative splicing and gene expression (Yan et al., 2015). Genomic coordinates in the output files were converted to mm9 with LiftOver (Kent et al., 2002). To identify stage-specific AS changes, available RNA-Seq datasets (Soumillon et al., 2013) were retrieved (GEO series: GSE43717) and processed as above. Significant AS changes were defined as those with FDR<0.05, *p.adj<0.05*. Overlapping AS events within each splicing category were collapsed and the ΔPSI values averaged, except for overlapping AS changes with opposite ΔPSI values that were discarded. The set of 217 genes with changes in cKO correspond to those with ΔPSI≥20 and an average RPKM>1 in cKO. To identify the 67 cassette exons, the coordinates of regulated cassette exons were intersected with BED files for each of the other five splicing types. Those cassette exons that did not overlap with a second splicing event were retained. The 988 genes with RPKM differences (p<0.01) in WT and cKO testes included those with RPKM>1 in WT and cKO.

HITS-CLIP

Testes from 8-week old mice were detunicated in cold HBSS and seminiferous tubules UV-irradiated on ice. Cross-linking, immunoprecipitation with anti-Ptbp2 (Polydorides et al., 2000), and cDNA library construction steps were performed as previously described (Licatalosi et al., 2008; Licatalosi et al., 2012). Libraries were generated from three biologic replicate animals and sequenced at the CWRU Sequencing Core. Reads were mapped to the

mm9 genome with Bowtie and collapsed to identify unique CLIP tags. CLIP clusters were identified using tools from Galaxy (Giardine et al., 2005), the UCSC Table Browser (Kent et al., 2002), BEDTools (Quinlan and Hall, 2010), and R. To identify BR3 clusters that map to RefSeq genes, overlapping RefSeq genes on the same strand were first collapsed to identify 22,308 merged genes (or transcription units, TUs). BR3 clusters were joined with TUs on the same strands, identifying 24,034 BR3 clusters that overlapped with 5,397 TUs. The distribution of BR3 clusters in intergenic and genic regions was assessed by intersection with RefSeq coding sequences (CDS), introns, and 5' and 3' UTRs retrieved from the UCSC Table Browser. BR3 clusters that mapped to a sequence with more than one type of annotation were labeled 'ambiguous'. To assess the distribution of clusters relative to splice sites, only BR3 clusters mapping to a single RefSeq intron were analyzed. PhastCons scores were retrieved for 29,206 BR3 clusters using the UCSC Table browser and used to calculate an average score per nucleotide of each cluster. Motif enrichment analyses were performed using the EMBOSS tools Compseq and Shuffleseq. The control set of constitutively spliced exons was obtained by randomly selecting internal exons pre-filtered for no overlap with annotated alternatively spliced exons.

Gene Ontology

GO term analyses were performed with the Cytoscape application BiNGO (Saito et al., 2012; Cline et al., 2007) using a hypergeometric statistical test and Benjamini & Hochberg FDR correction (significance level of 0.05) to identify enriched terms after multiple testing correction. To assess enriched terms associated with Ptbp2-regulated genes, the gene *Jmjd6* was omitted due to mis-annotation (Böttger et al., 2015). A custom set of background genes was generated consisting of 14,449 genes with RPKM >1 in P25 WT or cKO. Only enriched GO terms with at least 5 genes were considered. Similarly, custom background sets were generated for the analysis of enriched GO terms associated with T1, T2, and T3 (14,708, 11,871, and 14,091 genes, respectively).

Microscopy

Cryosections were processed for fluorescence microscopy following a published protocol (Li et al., 2013). For F-actin staining, cryosections were rinsed with PBS, permeabilized, and blocked with 5% normal goat serum. Sections were incubated with phalloidin (Molecular Probes), washed, and incubated with Lectin PNA (Molecular Probes) or antibody to Ddx4 (Abcam).

Supplementary Material

Refer to Web version on PubMed Central for supplementary material.

Acknowledgments

We are grateful to the following individuals for their contributions to this work: Douglas Black for providing mice with the *Ptbp2*^{flox} allele; Robert Darnell for Ptbp2 antibody; Sebastien Weyn-Vanhentenryck and Chaolin Zhang for assistance with OLego and Quantas; the CWRU Genomics Core for sequencing; the CWRU Virology, Next Generation Sequencing, and Imaging Core for microscopy; the CWRU Tissue Resources Core for sectioning; and Christopher Geyer and Jo Ann Wise for critical comments on the manuscript. This work was supported by NIH grant GM107331 to D.D.L.

References

Bi J, Li Y, Sun F, Saalbach A, Klein C, Miller DJ, Hess R, Nowak RA. Basigin null mutant male mice are sterile and exhibit impaired interactions between germ cells and Sertoli cells. Dev Biol. 2013; 380:145–156. [PubMed: 23727514]

Böttger A, Islam MS, Chowdhury R, Schofield CJ, Wolf A. The oxygenase Jmjd6--a case study in conflicting assignments. Biochem J. 2015; 468:191–202. [PubMed: 25997831]

Boutz PL, Stoilov P, Li Q, Lin CH, Chawla G, Ostrow K, Shiue L, Ares MJ, Black DL. A post-transcriptional regulatory switch in polypyrimidine tract-binding proteins reprograms alternative splicing in developing neurons. Genes Dev. 2007; 21:1636–1652. [PubMed: 17606642]

Cheng CY, Wong EW, Lie PP, Mruk DD, Xiao X, Li MW, Lui WY, Lee WM. Polarity proteins and actin regulatory proteins are unlikely partners that regulate cell adhesion in the seminiferous epithelium during spermatogenesis. Histol Histopathol. 2011; 26:1465–1474. [PubMed: 21938683]

Clark TA, Schweitzer AC, Chen TX, Staples MK, Lu G, Wang H, Williams A, Blume JE. Discovery of tissue-specific exons using comprehensive human exon microarrays. Genome Biol. 2007; 8:R64. [PubMed: 17456239]

Cline MS, Smoot M, Cerami E, Kuchinsky A, Landys N, Workman C, Christmas R, Avila-Campilo I, Creech M, Gross B, Hanspers K, Isserlin R, Kelley R, Killcoyne S, Lotia S, Maere S, Morris J, Ono K, Pavlovic V, Pico AR, Vailaya A, Wang PL, Adler A, Conklin BR, Hood L, Kuiper M, Sander C, Schmulevich I, Schwikowski B, Warner GJ, Ideker T, Bader GD. Integration of biological networks and gene expression data using Cytoscape. Nat Protoc. 2007; 2:2366–2382. [PubMed: 17947979]

Dong H, Chen Z, Wang C, Xiong Z, Zhao W, Jia C, Lin J, Lin Y, Yuan W, Zhao AZ, Bai X. Rictor Regulates Spermatogenesis by Controlling Sertoli Cell Cytoskeletal Organization and Cell Polarity in the Mouse Testis. Endocrinology. 2015; 156:4244–4256. [PubMed: 26360620]

Ehrmann I, Elliott DJ. Expression and functions of the star proteins Sam68 and T-STAR in mammalian spermatogenesis. Adv Exp Med Biol. 2010; 693:67–81. [PubMed: 21189686]

Fu XD, Ares MJ. Context-dependent control of alternative splicing by RNA-binding proteins. Nat Rev Genet. 2014; 15:689–701. [PubMed: 25112293]

Giardine B, Riemer C, Hardison RC, Burhans R, Elnitski L, Shah P, Zhang Y, Blankenberg D, Albert I, Taylor J, Miller W, Kent WJ, Nekrutenko A. Galaxy: a platform for interactive large-scale genome analysis. Genome Res. 2005; 15:1451–1455. [PubMed: 16169926]

Griswold MD. The central role of Sertoli cells in spermatogenesis. Semin Cell Dev Biol. 1998; 9:411–416. [PubMed: 9813187]

Johnson GD, Lalancette C, Linnemann AK, Leduc F, Boissonneault G, Krawetz SA. The sperm nucleus: chromatin, RNA, and the nuclear matrix. Reproduction. 2011; 141:21–36. [PubMed: 20876223]

Johnson KJ. Testicular histopathology associated with disruption of the Sertoli cell cytoskeleton. Spermatogenesis. 2014; 4:e979106. [PubMed: 26413393]

Kent WJ, Sugnet CW, Furey TS, Roskin KM, Pringle TH, Zahler AM, Haussler D. The human genome browser at UCSC. Genome Res. 2002; 12:996–1006. [PubMed: 12045153]

Keppetipola N, Sharma S, Li Q, Black DL. Neuronal regulation of pre-mRNA splicing by polypyrimidine tract binding proteins, PTBP1 and PTBP2. Crit Rev Biochem Mol Biol. 2012; 47:360–378. [PubMed: 22655688]

Kleene KC. Connecting cis-elements and trans-factors with mechanisms of developmental regulation of mRNA translation in meiotic and haploid mammalian spermatogenic cells. Reproduction. 2013; 146:R1–19. [PubMed: 23579190]

Konig J, Zarnack K, Luscombe NM, Ule J. Protein-RNA interactions: new genomic technologies and perspectives. Nat Rev Genet. 2011; 13:77–83.

Kress C, Gautier-Courteille C, Osborne HB, Babinet C, Paillard L. Inactivation of CUG-BP1/CELF1 causes growth, viability, and spermatogenesis defects in mice. Mol Cell Biol. 2007; 27:1146–1157. [PubMed: 17130239]

Kühn S, Geyer M. Formins as effector proteins of Rho GTPases. Small GTPases. 2014; 5:e29513. [PubMed: 24914801]

Li Q, Zheng S, Han A, Lin CH, Stoilov P, Fu XD, Black DL. The splicing regulator PTBP2 controls a program of embryonic splicing required for neuronal maturation. Elife. 2014; 3:e01201. [PubMed: 24448406]

Li X, Mao Z, Wu M, Xia J. Rescuing infertility of Pick1 knockout mice by generating testis-specific transgenic mice via testicular infection. Sci Rep. 2013; 3:2842. [PubMed: 24100262]

Licatalosi DD. Roles of RNA-binding Proteins and Post-transcriptional Regulation in Driving Male Germ Cell Development in the Mouse. Adv Exp Med Biol. 2016; 907:123–151. [PubMed: 27256385]

Licatalosi DD, Darnell RB. RNA processing and its regulation: global insights into biological networks. Nat Rev Genet. 2010; 11:75–87. [PubMed: 20019688]

Licatalosi DD, Mele A, Fak JJ, Ule J, Kayikci M, Chi SW, Clark TA, Schweitzer AC, Blume JE, Wang X, Darnell JC, Darnell RB. HITS-CLIP yields genome-wide insights into brain alternative RNA processing. Nature. 2008; 456:464–469. [PubMed: 18978773]

Licatalosi DD, Yano M, Fak JJ, Mele A, Grabinski SE, Zhang C, Darnell RB. Ptbp2 represses adult-specific splicing to regulate the generation of neuronal precursors in the embryonic brain. Genes Dev. 2012; 26:1626–1642. [PubMed: 22802532]

Lie PP, Mruk DD, Lee WM, Cheng CY. Cytoskeletal dynamics and spermatogenesis. Philos Trans R Soc Lond B Biol Sci. 2010; 365:1581–1592. [PubMed: 20403871]

Lillevali K, Kulla A, Ord T. Comparative expression analysis of the genes encoding polypyrimidine tract binding protein (PTB) and its neural homologue (brPTB) in prenatal and postnatal mouse brain. Mech Dev. 2001; 101:217–220. [PubMed: 11231079]

Lui WY, Mruk DD, Cheng CY. Interactions among IQGAP1, Cdc42, and the cadherin/catenin protein complex regulate Sertoli-germ cell adherens junction dynamics in the testis. J Cell Physiol. 2005; 202:49–66. [PubMed: 15389538]

Makeyev EV, Zhang J, Carrasco MA, Maniatis T. The MicroRNA miR-124 promotes neuronal differentiation by triggering brain-specific alternative pre-mRNA splicing. Mol Cell. 2007; 27:435–448. [PubMed: 17679093]

Marat AL, Dokainish H, McPherson PS. DENN domain proteins: regulators of Rab GTPases. J Biol Chem. 2011; 286:13791–13800. [PubMed: 21330364]

Mellman I, Nelson WJ. Coordinated protein sorting, targeting and distribution in polarized cells. Nat Rev Mol Cell Biol. 2008; 9:833–845. [PubMed: 18946473]

Merkin J, Russell C, Chen P, Burge CB. Evolutionary dynamics of gene and isoform regulation in Mammalian tissues. Science. 2012; 338:1593–1599. [PubMed: 23258891]

Nakata H, Wakayama T, Takai Y, Iseki S. Quantitative analysis of the cellular composition in seminiferous tubules in normal and genetically modified infertile mice. J Histochem Cytochem. 2015; 63:99–113. [PubMed: 25411188]

O'Bryan MK, Clark BJ, McLaughlin EA, D'Sylva RJ, O'Donnell L, Wilce JA, Sutherland J, O'Connor AE, Whittle B, Goodnow CC, Ormandy CJ, Jamsai D. RBM5 is a male germ cell splicing factor and is required for spermatid differentiation and male fertility. PLoS Genet. 2013; 9:e1003628. [PubMed: 23935508]

Oberstrass FC, Auweter SD, Erat M, Hargous Y, Henning A, Wenter P, Reymond L, Amir-Ahmady B, Pitsch S, Black DL, Allain FH. Structure of PTB bound to RNA: specific binding and implications for splicing regulation. Science. 2005; 309:2054–2057. [PubMed: 16179478]

Obholz KL, Akopyan A, Waymire KG, MacGregor GR. FNDC3A is required for adhesion between spermatids and Sertoli cells. Dev Biol. 2006; 298:498–513. [PubMed: 16904100]

Parsons JT, Horwitz AR, Schwartz MA. Cell adhesion: integrating cytoskeletal dynamics and cellular tension. Nat Rev Mol Cell Biol. 2010; 11:633–643. [PubMed: 20729930]

Polydorides AD, Okano HJ, Yang YY, Stefani G, Darnell RB. A brain-enriched polypyrimidine tract-binding protein antagonizes the ability of Nova to regulate neuron-specific alternative splicing. Proc Natl Acad Sci U S A. 2000; 97:6350–5. [PubMed: 10829067]

Quinlan AR, Hall IM. BEDTools: a flexible suite of utilities for comparing genomic features. Bioinformatics. 2010; 26:841–842. [PubMed: 20110278]

Ramskold D, Wang ET, Burge CB, Sandberg R. An abundance of ubiquitously expressed genes revealed by tissue transcriptome sequence data. PLoS Comput Biol. 2009; 5:e1000598. [PubMed: 20011106]

Saito R, Smoot ME, Ono K, Ruscheinski J, Wang PL, Lotia S, Pico AR, Bader GD, Ideker T. A travel guide to Cytoscape plugins. Nat Methods. 2012; 9:1069–1076. [PubMed: 23132118]

Sawicka K, Bushell M, Spriggs KA, Willis AE. Polypyrimidine-tract-binding protein: a multifunctional RNA-binding protein. Biochem Soc Trans. 2008; 36:641–647. [PubMed: 18631133]

Schmid R, Grellscheid SN, Ehrmann I, Dalgliesh C, Danilenko M, Paronetto MP, Pedrotti S, Grellscheid D, Dixon RJ, Sette C, Eperon IC, Elliott DJ. The splicing landscape is globally reprogrammed during male meiosis. Nucleic Acids Res. 2013; 41:10170–10184. [PubMed: 24038356]

Scotti MM, Swanson MS. RNA mis-splicing in disease. Nat Rev Genet. 2016; 17:19–32. [PubMed: 26593421]

Sette C, Messina V, Paronetto MP. Sam68: a new STAR in the male fertility firmament. J Androl. 2010; 31:66–74. [PubMed: 19875495]

Sharma S, Falick AM, Black DL. Polypyrimidine tract binding protein blocks the 5' splice site-dependent assembly of U2AF and the prespliceosomal E complex. Mol Cell. 2005; 19:485–496. [PubMed: 16109373]

Sharma S, Maris C, Allain FH, Black DL. U1 snRNA directly interacts with polypyrimidine tract-binding protein during splicing repression. Mol Cell. 2011; 41:579–588. [PubMed: 21362553]

Shen S, Park JW, Huang J, Dittmar KA, Lu ZX, Zhou Q, Carstens RP, Xing Y. MATS: a Bayesian framework for flexible detection of differential alternative splicing from RNA-Seq data. Nucleic Acids Res. 2012; 40:e61. [PubMed: 22266656]

Soumillon M, Necsulea A, Weier M, Brawand D, Zhang X, Gu H, Barthes P, Kokkinaki M, Nef S, Gnirke A, Dym M, de Massy B, Mikkelsen TS, Kaessmann H. Cellular source and mechanisms of high transcriptome complexity in the mammalian testis. Cell Rep. 2013; 3:2179–2190. [PubMed: 23791531]

Spellman R, Llorian M, Smith CW. Crossregulation and functional redundancy between the splicing regulator PTB and its paralogs nPTB and ROD1. Mol Cell. 2007; 27:420–434. [PubMed: 17679092]

Spellman R, Smith CW. Novel modes of splicing repression by PTB. Trends Biochem Sci. 2006; 31:73–76. [PubMed: 16403634]

Tang EI, Lee WM, Cheng CY. Coordination of Actin- and Microtubule-Based Cytoskeletons Supports Transport of Spermatids and Residual Bodies/Phagosomes During Spermatogenesis in the Rat Testis. Endocrinology. 2016; 157:1644–1659. [PubMed: 26894662]

Tanwar PS, Kaneko-Tarui T, Zhang L, Teixeira JM. Altered LKB1/AMPK/TSC1/TSC2/mTOR signaling causes disruption of Sertoli cell polarity and spermatogenesis. Hum Mol Genet. 2012; 21:4394–4405. [PubMed: 22791749]

Tanwar PS, Zhang L, Teixeira JM. Adenomatous polyposis coli (APC) is essential for maintaining the integrity of the seminiferous epithelium. Mol Endocrinol. 2011; 25:1725–1739. [PubMed: 21816903]

The UniProt Consortium. UniProt: the universal protein knowledgebase. Nucleic Acids Res. 2016

Trapnell C, Roberts A, Goff L, Pertea G, Kim D, Kelley DR, Pimentel H, Salzberg SL, Rinn JL, Pachter L. Differential gene and transcript expression analysis of RNA-seq experiments with TopHat and Cufflinks. Nat Protoc. 2012; 7:562–578. [PubMed: 22383036]

van der Weyden L, Arends MJ, Chausiaux OE, Ellis PJ, Lange UC, Surani MA, Affara N, Murakami Y, Adams DJ, Bradley A. Loss of TSLC1 causes male infertility due to a defect at the spermatid stage of spermatogenesis. Mol Cell Biol. 2006; 26:3595–3609. [PubMed: 16611999]

Vogl AW, Vaid KS, Guttman JA. The Sertoli cell cytoskeleton. Adv Exp Med Biol. 2008; 636:186–211. [PubMed: 19856169]

Voung JK, Lin CH, Zhang M, Chen L, Black DL, Zheng S. PTBP1 and PTBP2 serve both specific and redundant functions in neuronal pre-mRNA splicing. Cell Rep. 2016; 17:2766–2775. [PubMed: 27926877]

Wallar BJ, Stropich BN, Schoenherr JA, Holman HA, Kitchen SM, Alberts AS. The basic region of the diaphanous-autoregulatory domain (DAD) is required for autoregulatory interactions with the diaphanous-related formin inhibitory domain. J Biol Chem. 2006; 281:4300–4307. [PubMed: 16361707]

Watanabe T, Wang S, Kaibuchi K. IQGAPs as Key Regulators of Actin-cytoskeleton Dynamics. Cell Struct Funct. 2015; 40:69–77. [PubMed: 26051604]

West JJ, Harris TJ. Cadherin Trafficking for Tissue Morphogenesis: Control and Consequences. Traffic. 2016; 17:1233–1243. [PubMed: 27105637]

Wu J, Anczukow O, Krainer AR, Zhang MQ, Zhang C. OLego: fast and sensitive mapping of spliced mRNA-Seq reads using small seeds. Nucleic Acids Res. 2013; 41:5149–5163. [PubMed: 23571760]

Xu M, Hecht NB. Polypyrimidine tract binding protein 2 stabilizes phosphoglycerate kinase 2 mRNA in murine male germ cells by binding to its 3'UTR. Biol Reprod. 2007; 76:1025–1033. [PubMed: 17329592]

Yamada D, Yoshida M, Williams YN, Fukami T, Kikuchi S, Masuda M, Maruyama T, Ohta T, Nakae D, Maekawa A, Kitamura T, Murakami Y. Disruption of spermatogenic cell adhesion and male infertility in mice lacking TSLC1/IGSF4, an immunoglobulin superfamily cell adhesion molecule. Mol Cell Biol. 2006; 26:3610–3624. [PubMed: 16612000]

Yan Q, Weyn-Vanhentenryck SM, Wu J, Sloan SA, Zhang Y, Chen K, Wu JQ, Barres BA, Zhang C. Systematic discovery of regulated and conserved alternative exons in the mammalian brain reveals NMD modulating chromatin regulators. Proc Natl Acad Sci U S A. 2015; 112:3445–3450. [PubMed: 25737549]

Yap K, Xiao Y, Friedman BA, Je HS, Makeyev EV. Polarizing the Neuron through Sustained Co-expression of Alternatively Spliced Isoforms. Cell Rep. 2016; 15:1316–1328. [PubMed: 27134173]

Yeo G, Holste D, Kreiman G, Burge CB. Variation in alternative splicing across human tissues. Genome Biol. 2004; 5:R74. [PubMed: 15461793]

Zagore LL, Grabinski SE, Sweet TJ, Hannigan MM, Sramkoski RM, Li Q, Licatalosi DD. RNA Binding Protein Ptbp2 Is Essential for Male Germ Cell Development. Mol Cell Biol. 2015; 35:4030–4042. [PubMed: 26391954]

Zhapparova ON, Fokin AI, Vorobyeva NE, Bryantseva SA, Nadezhdina ES. Ste20-like protein kinase SLK (LOSK) regulates microtubule organization by targeting dynactin to the centrosome. Mol Biol Cell. 2013; 24:3205–3214. [PubMed: 23985322]

Zheng S, Gray EE, Chawla G, Porse BT, O'Dell TJ, Black DL. PSD-95 is post-transcriptionally repressed during early neural development by PTBP1 and PTBP2. Nat Neurosci. 2012; 15:381–8. S1. [PubMed: 22246437]

Highlights

- Alternative splicing is regulated in a stage-specific manner during spermatogenesis
- Ptbp2 is a critical regulator of alternative splicing during germ cell development
- Ptbp2 controls a network of trafficking and cell adhesion genes via exon repression
- Germ-Sertoli cell crosstalk requires Ptbp2 expression in germ cells

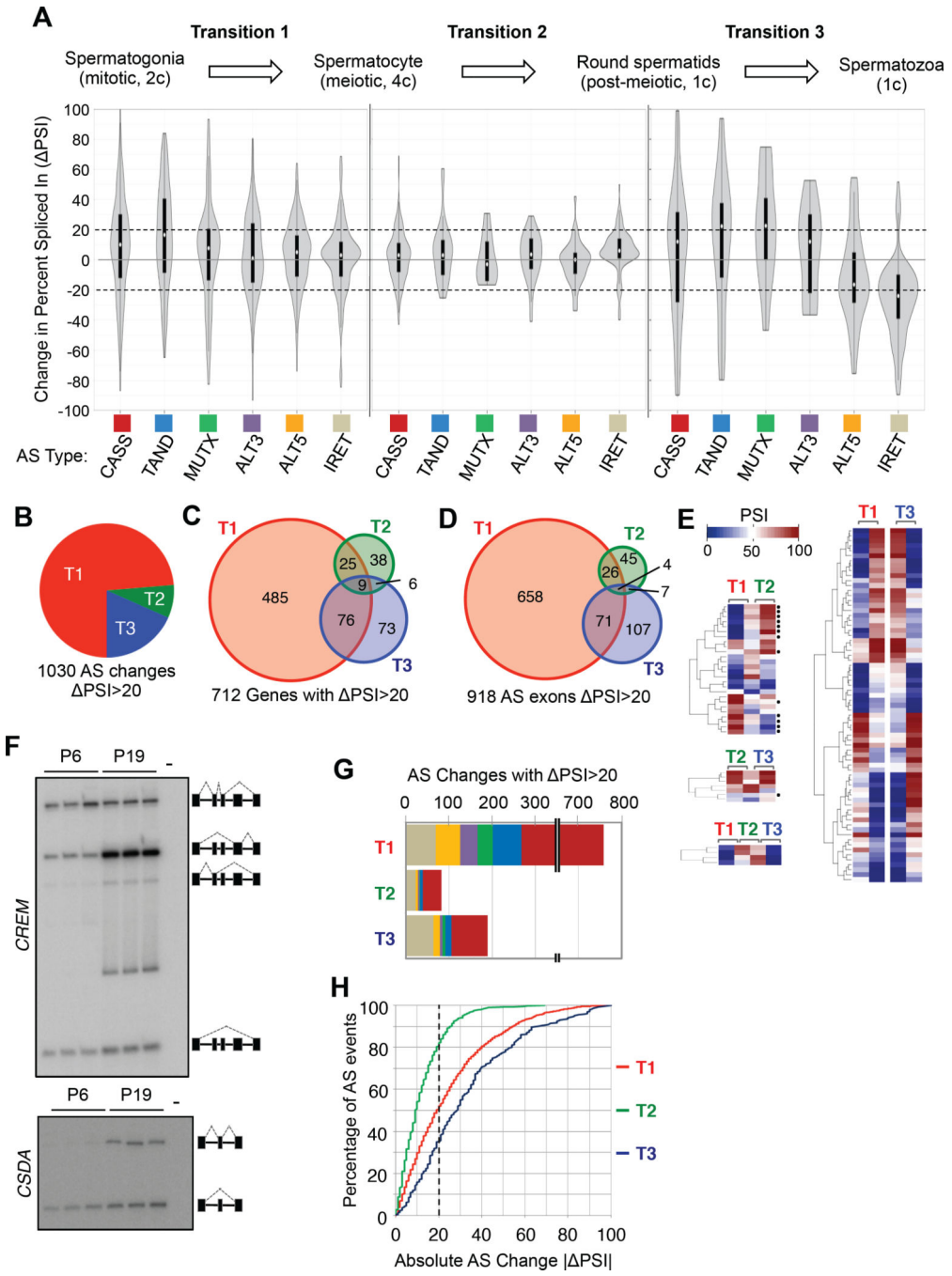

Figure 1.

Identification of stage-specific AS changes in spermatogenesis. (A) Top: Schematic of the three pairwise comparisons of cell types (transitions) examined. Bottom: Violin plots showing the distribution of ΔPSI values (FDR<0.05 and p<0.05) for each AS category in transition 1, 2, and 3 (left, center, and right, respectively). Dashed lines are positioned at ΔPSI=±20%. AS type is indicated at the bottom. (B) Pie chart showing the distribution of AS changes detected in each transition. (C) Number and overlap in genes with AS changes in one or more transitions. (D) Number and overlap in individual AS exons with changes in

one or more transitions. (E) Clustered heatmaps showing PSI values of AS exons regulated in more than one transition (overlapping events from panel D), indicated by the blue/red color scale. Each column represents a single cell type in the transitions that are being compared, while each row represents an overlapping AS exon. Black dots represent an AS exon that undergoes a unidirectional, continuous splicing change. (F) Representative examples of RT-PCR validation of splicing changes measured in triplicate in P6 and P19 testes. (G) Bar chart showing the number of AS changes (ΔPSI=±20%) for each AS category in each transition. Color code for each AS type is indicated in A. (H) Distribution of absolute ΔPSI values in T1, T2, and T3. Dashed line represents ΔPSI>±20%. See also Figures S1,2; Tables S1,3; Files S1,4.

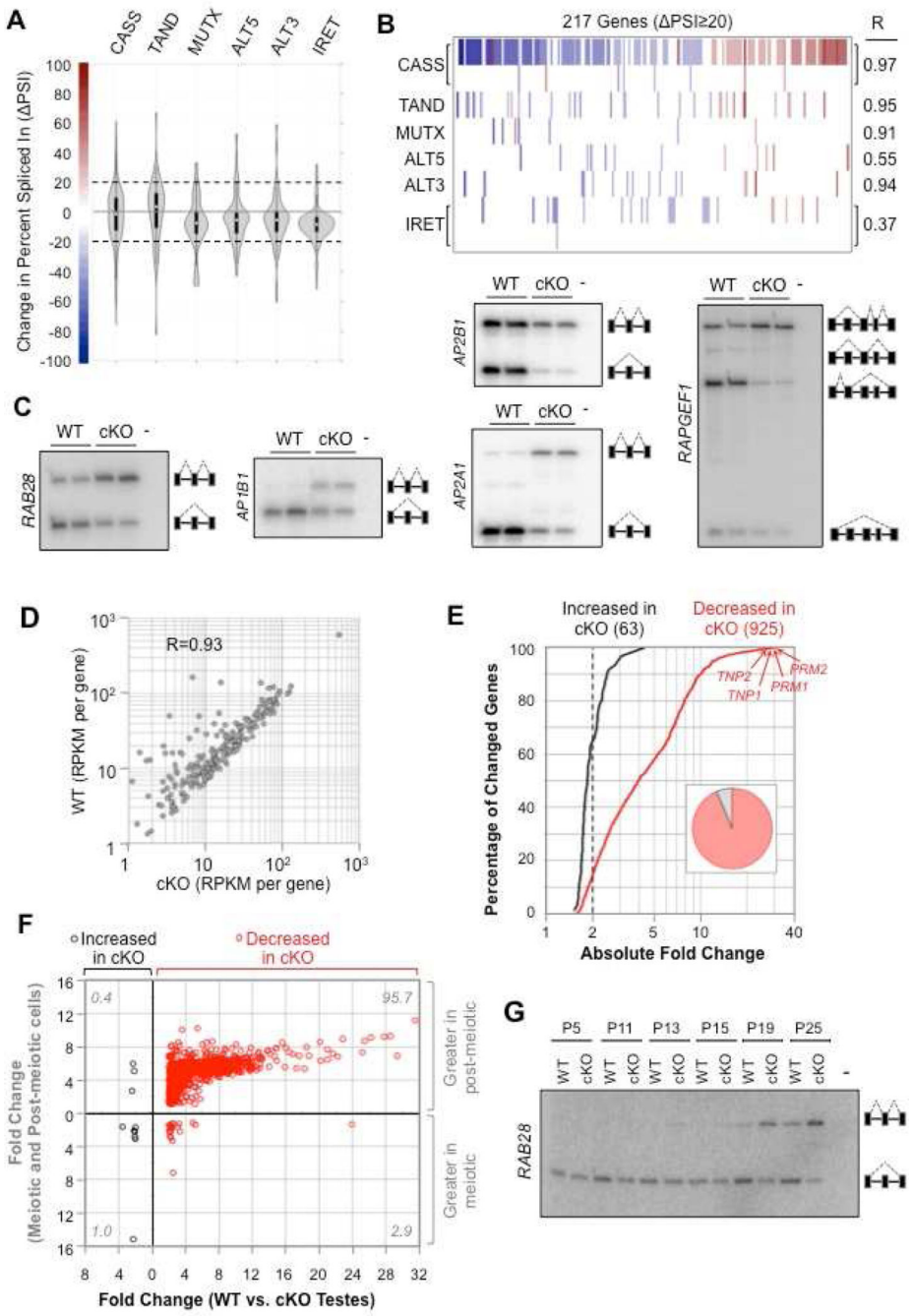

Figure 2.

Identification of AS differences between WT and cKO testes. (A) Violin plots showing the distribution of ΔPSI values for each splicing category. (B) 257 AS changes with ΔPSI>20 in 217 genes, binned according to the splicing categories indicated at left. Color-coding reflects ΔPSI value, according to the gradient shown in A. Pearson correlation coefficients (R) are shown at right for RPKM comparisons in WT and cKO for genes with AS changes in each category. (C) Representative examples of RT-PCR analysis of AS isoforms measured in replicate WT and cKO testes at P25. (D) Comparison of RPKM values for the 217 genes

with ΔPSI=±20% AS changes in WT and cKO testes. (E) Distribution of absolute fold change fold change values for genes with RNA increases or decreases in cKO testes (black and red lines, respectively). Dashed line is positioned at absolute fold change of 2. Inset shows relative number of genes with RNA increases (grey) or decreases (red). (F) Comparison of fold change values for the 792 RNAs that shared 2-fold or greater differences ($p<0.01$) in analysis of both WT versus cKO (x-axis) and meiotic versus post-meiotic cells (y-axis). Values in each corner correspond to the percentage of data points in each quadrant. (G) Representative example of RT-PCR validation of an AS event that is stage-specific and Ptbp2-dependent, with postnatal age of tissue indicated at top. See also Figure S3; Tables S2,3; Files S1,2

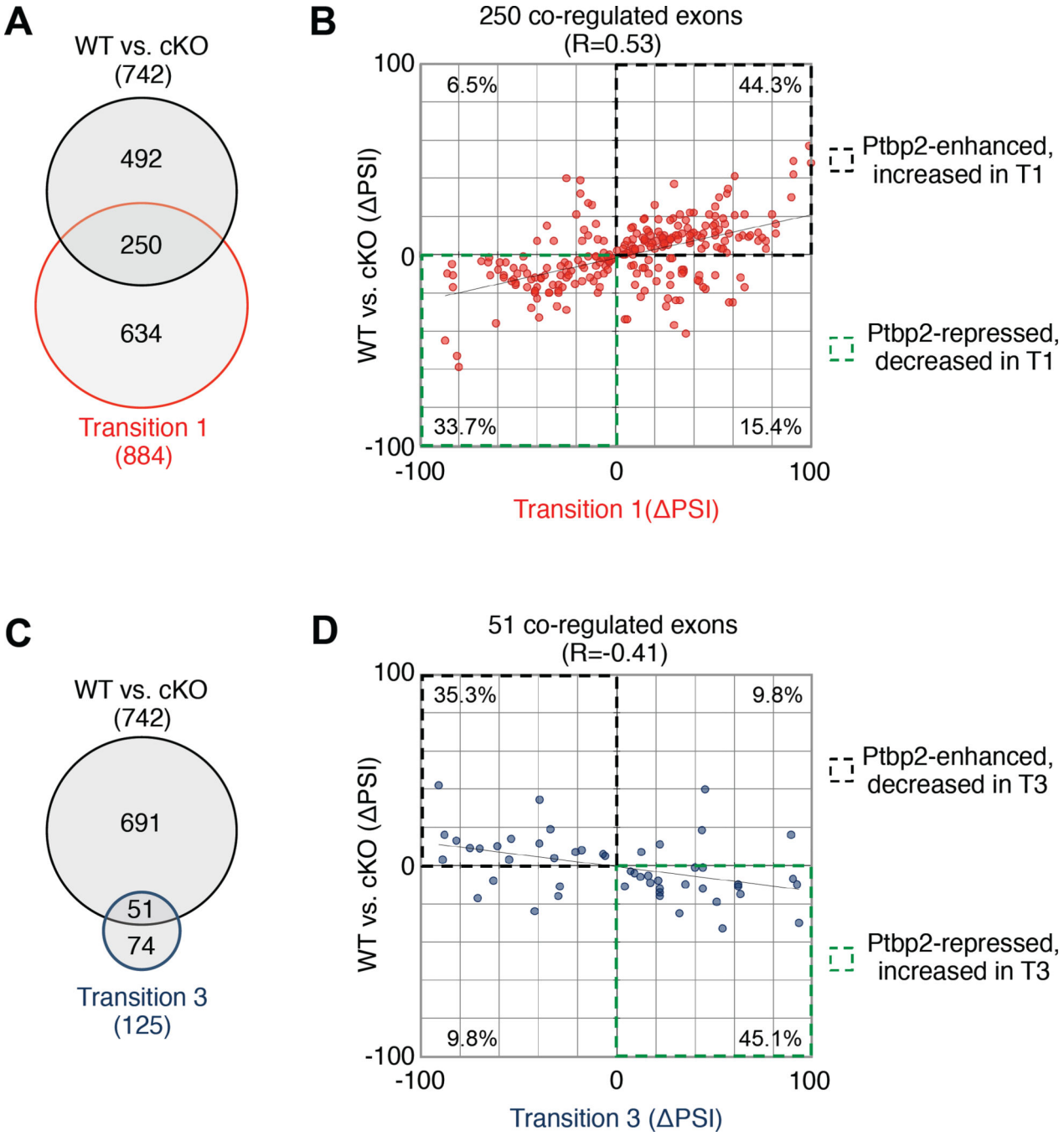

Figure 3.

Ptbp2 regulates AS temporally (A) Intersection of AS cassette exons identified in T1 and in WT versus cKO datasets. (B) Distribution of ΔPSI values for 250 co-regulated cassette exons indicated in A. (C) Intersection of AS cassette exons identified in T3 and in WT versus cKO datasets. (D) Distribution of ΔPSI values for 51 co-regulated cassette exons indicated in C.

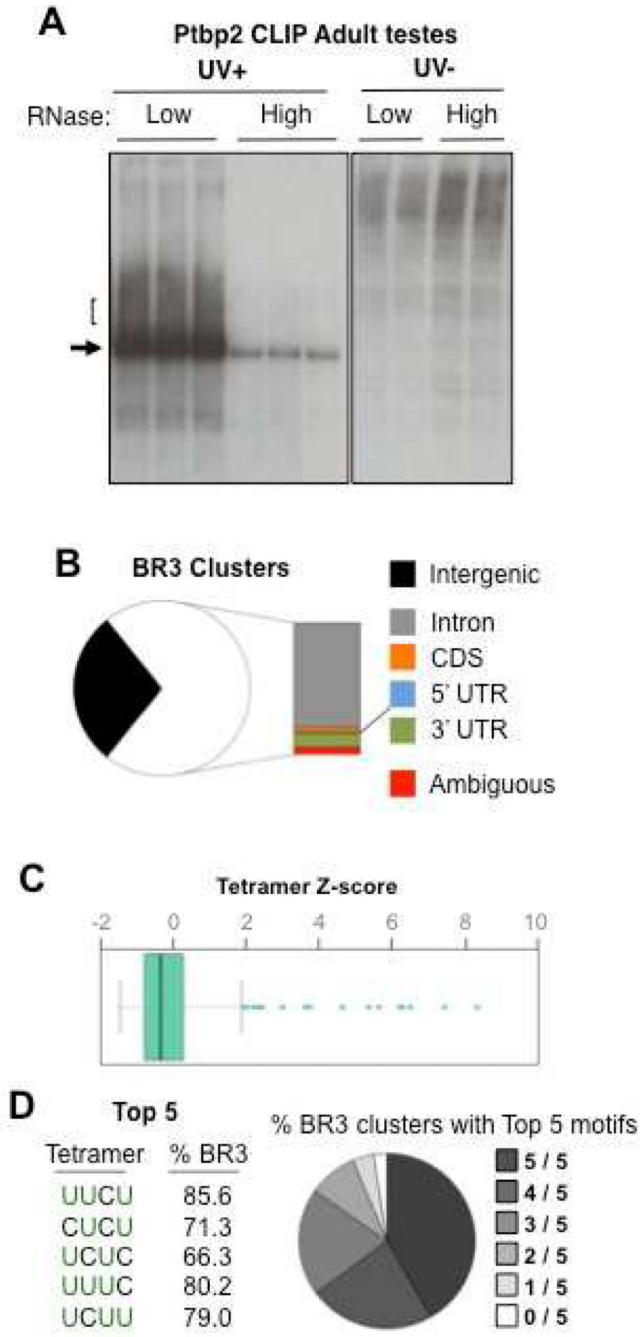

Figure 4.

Identification of Ptbp2 binding sites in the germ cell transcriptome. (A) Autorad of nitrocellulose membrane containing cross-linked and radiolabelled Ptbp2-RNA complexes immunopurified from lysates treated with either a high (1:1,000) or low (1:20,000) concentration of RNAse. Assays were performed in parallel using UV-irradiated and non-irradiated testes (UV+ and UV-, respectively). Arrow denotes position of Ptbp2. Open bracket indicates region of membrane excised for library preparation. (B) Distribution of BR3 clusters in intergenic and genic regions. CDS corresponds to exonic coding sequences,

while ambiguous BR3 clusters are those that map to sequences with more than one annotation. (C) Distribution of z-scores following tetramer-enrichment analysis for BR3 clusters. (D) Motifs with the top 5 z-scores are shown at top, with the percentage of BR3 clusters containing each motif indicated. Pie chart indicates the percentage of clusters that contain one or more of the top 5 motifs. See also Figure S6; File S3

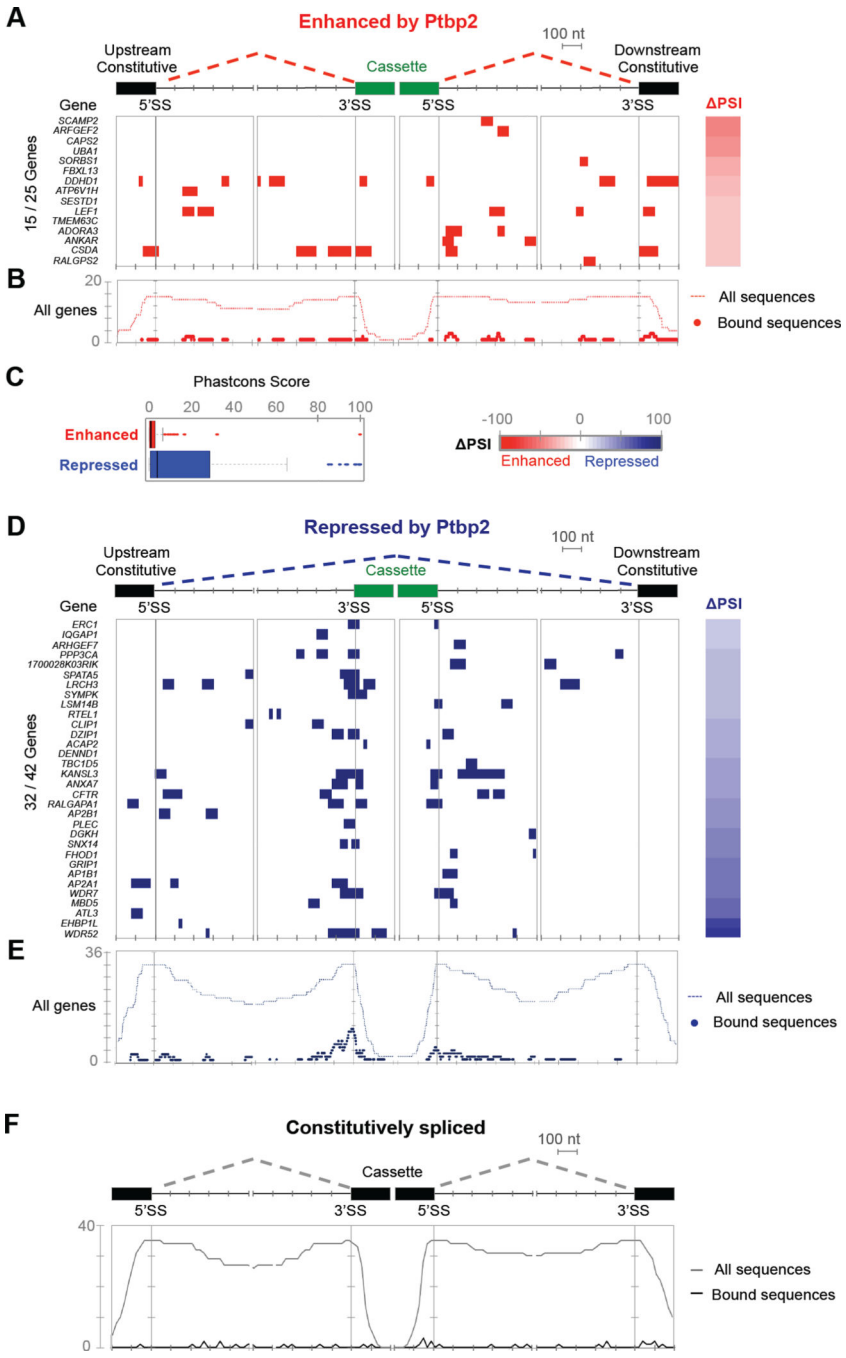

Figure 5.

Analysis of Ptbp2-RNA interactions near cassette exons. Distribution of binding sites in 20 nt windows relative to the splice sites of the Ptbp2-enhanced (A, red boxes) and Ptbp2-repressed (D, blue boxes) cassette exons and the 5' and 3'splice sites of the upstream and downstream constitutively spliced exons, respectively. Each row in A and D represents a cassette exon region, with some rows empty due to the absence of a Ptbp2-RNA interaction within the intervals included in the figure. Metagene summaries of the data in A and D are shown in panels B and E, wherein thick dots indicate number of binding events relative to

the indicated splice sites, and the dotted lines represent the number of regions that have exons or introns of the indicated size. (C) Distribution of PhastCons scores for Ptbp2-RNA interactions in regions associated with Ptbp2-enhanced (red) and Ptbp2-repressed cassette exons. (F) Metagene analysis of Ptbp2 binding events in a control set of 100 randomly selected internal coding exons, with 35 containing BR2 or BR3 sites. Black line represents the number of Ptbp2 binding events relative to the indicated splice sites, while grey lines represent the number of regions that have exons or introns of the indicated size. See also File S3

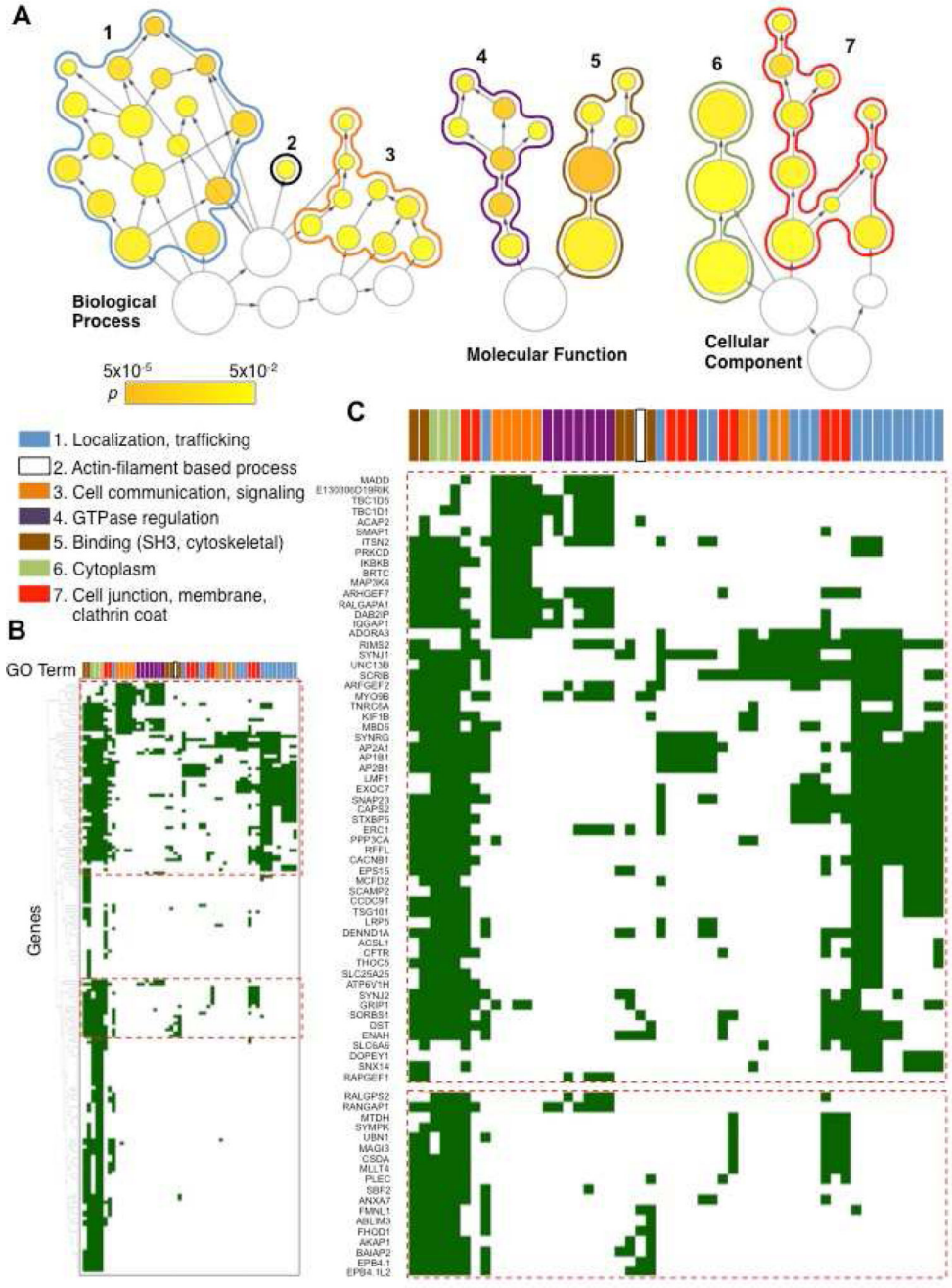

Figure 6.

Enriched gene ontology terms associated with RNAs that are mis-spliced in *Ptbp2*-deficient testes. (A) Hierarchical view of parent-child relationships for the enriched GO terms associated with genes with altered AS in cKO testis. Seven different groups were identified and outlined to match colors assigned to each group indicated at bottom. Circle sizes reflect the number of genes in each enriched term, while circle color reflects enrichment *p* value. (B) Clustering of genes based on co-occurrence in the enriched GO terms, with color-coded

GO terms indicated at the top. (C) Higher magnification view of two boxed regions (dotted lines) from B. See also Figure S4; File S4

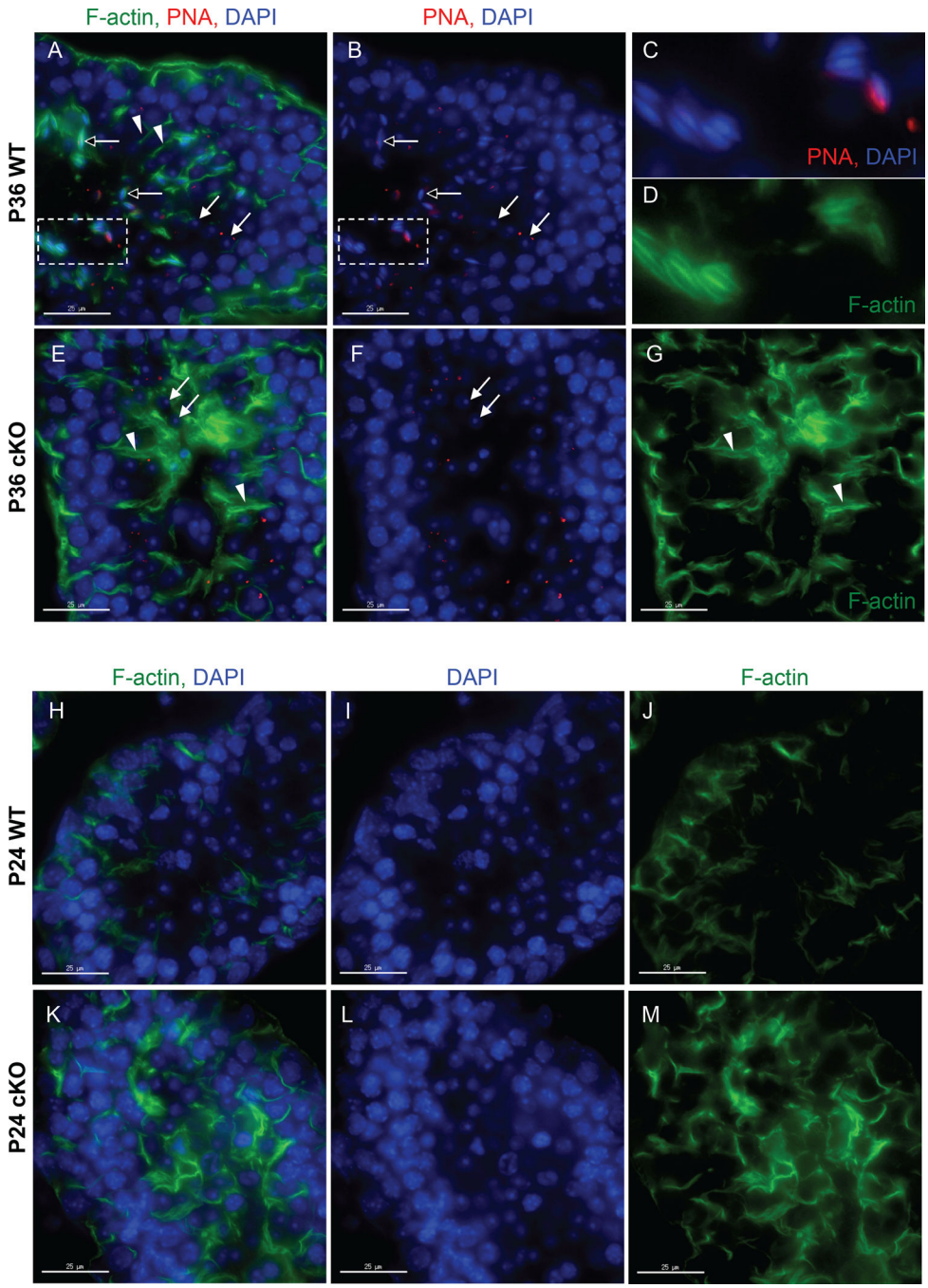

Figure 7.

Ptbp2-loss in germ cells results in disorganization of the Sertoli cell actin cytoskeleton. Fluorescence microscopy to detect F-actin (phalloidin, green), acrosome (PNA, red), and DNA (DAPI, blue). A-D shows a representative seminiferous tubule from a P36 WT mouse, with panels C and D showing high magnification views of the dotted box in A and B which contains elongated spermatids. E-G shows a representative example from a P36 cKO seminiferous tubules. H-J and K-M show representative examples of seminiferous tubules from P24 WT and cKO mice, respectively. Open arrows indicate elongated spermatids,

closed arrows indicate early round spermatids, and arrowheads indicate polarized F-actin filaments. Scale bar is 25 μM. See also Figure S5